Protein Synthesis Blockade Prevents Fear Memory Reactivation via Inhibition of Engram Synapse Strengthening

Ilgang Hong[1,2,*], Yeonjun Kim[1,2,*], Hyunsu Jung[1,2], Chang-Ho Kim[1,3], Jun-Hyeong Cho[4], Bong-Kiun Kaang[1,2,3]

[1]Center for Cognition and Sociality, Institute for Basic Science (IBS), Daejeon, South Korea
[2]Interdisciplinary Program in Neuroscience, Seoul National University, Seoul, South Korea
[3]Department of Biological Sciences, College of Natural Sciences, Seoul National University, Seoul, South Korea
[4]Department of Molecular, Cell and Systems Biology, University of California, Riverside, CA, USA

*These authors contributed equally.
Correspondence to: kaang@ibs.re.kr

Abstract

Memory relies on ensembles of engram cells in the brain. While previous studies have established the existence of these cells, the relationship between cellular and synaptic activity remains unclear. To address this, we applied the dual e-GRASP technique in mice to examine synaptic connectivity between the ventral CA1 and the basal amygdala during memory formation. We found that contextual fear conditioning increased engram-to-engram synapse (engram synapse) density and induced structural potentiation, underscoring their importance in associative memory. Additionally, we investigated the role of protein synthesis in memory formation by inducing retrograde amnesia using anisomycin, a protein synthesis inhibitor. Mice injected with anisomycin once (1xANI) showed impaired natural recall but still displayed fear responses upon optogenetic reactivation of engram cells. In contrast, mice that received four anisomycin injections over six hours (4xANI) showed significantly impaired natural recall and failed to exhibit fear responses upon optogenetic reactivation. This behavioural phenotype was correlated with synaptic changes: 1xANI mice exhibited no significant reduction in engram synapse density but had significantly smaller spine sizes, whereas 4xANI mice showed both a significant reduction in engram synapse density and spine size. Our results indicate that protein synthesis inhibition significantly reduces engram synapse density and spine size, changes that correlate with reductions in fear memory during both natural recall and artificial reactivation.

Introduction

The concept of the engram refers to the physical trace of a memory, which operates across multiple scales[1]. Engrams have been studied at the synaptic level in various behavioural paradigms—including contextual fear conditioning, auditory fear conditioning, and motor learning—as well as across different memory stages, such as consolidation, extinction, and remote recall[2–5]. However, whether this hypothesis extends beyond the CA3-CA1 circuit in fear learning remains unclear. In this study, we explore the engram synapse hypothesis within the ventral CA1 (vCA1) – basal amygdala (BA) circuit during associative fear learning.

The vCA1 is known to play a critical role in aversive learning, with growing evidence suggesting that engram neurons within this region encode information essential for forming lasting associations such as linking a specific environment to an aversive outcome[6–8]. Conversely, the amygdala is widely recognised for its role in processing emotions, especially fear-related responses[9,10]. Within this framework, activated vCA1 neurons are thought to convey contextual representations to the BA. Although the anatomical and functional connectivity between vCA1 and BA has been demonstrated in both *ex vivo* and *in vivo* studies, direct visualization of this connection at the synaptic level remains largely unexplored.

Protein synthesis is known to be critical in long-lasting forms of synaptic plasticity[11,12]. Applying a protein synthesis inhibitor (PSI) such as cycloheximide or anisomycin in brain slices prior to tetanisation has been shown to reduce the amplitude of field excitatory postsynaptic potentials and impair synaptic transmission during the late phase of long-term potentiation[13–15]. Consequently, inhibiting protein synthesis during acquisition blocks natural recall[16]. As anticipated, the disruption of memory consolidation is accompanied by the loss of enhanced synaptic strength in engram cells[16,17].

61

62 Protein synthesis is essential for natural memory recall, but its role in memory storage and
63 artificial recall remains debated. A single anisomycin injection after memory acquisition
64 impairs natural recall, yet optogenetic reactivation of DG engram cells can still induce memory
65 retrieval[16]. However, when anisomycin is administered alongside tat-Beclin, an autophagy-
66 inducing drug, both natural and artificial recall are disrupted[18]. This raises the question of
67 whether memory storage and artificial recall are critically affected by the magnitude of protein
68 synthesis blockade. Additionally, the synaptic changes associated with protein synthesis
69 blockade remain unclear. Here, we demonstrate that in the vCA1-BA circuit, the impairment
70 of both natural recall and optogenetic reactivation depends on the degree of protein synthesis
71 inhibition, which correlates with reductions in engram synapse density and spine size.

72

73 ## Results

74 **Validation of vCA1-BA circuit during contextual fear memory**

75 The inner (stratum radiatum facing) and outer (stratum oriens facing) layers of vCA1 projecting
76 to the BA are known to play distinct roles in anxiogenic and anxiolytic behaviour, but also in
77 fear memory[6,19,20]. To determine which layer projects to the BA, retrograde viral tracing was
78 performed by injecting retrogradely transducing CAV-Cre into the BA of double-floxed
79 tdTomato mice. Retrograde tracing confirmed that BA-projecting vCA1 neurones mainly
80 reside in the outer layer (Fig. S1).

81

82 Next, to see whether each neurone can store fear memory as an engram cell, the reactivation
83 ratio between acquisition- and retrieval-activated cells was observed. Acquisition-activated
84 neurones were labelled using c-Fos promoter driven Tet-on system and recall-activated
85 neurones were labelled using c-Fos immunohistochemistry (Fig. S2 A, B). A significant

86 increase in colocalisation ratio was observed in the contextual fear conditioning (CFC) group
87 compared to the naïve group in both vCA1 and BA (Fig. S2 C-E).
88
89 **Increased synaptic density and spine size between vCA1 and BA engram cells during**
90 **memory formation**
91 Next, correlation between associative memory formation and synaptic connectivity between
92 engram cells was assessed. Dual enhanced green fluorescent protein reconstitution across
93 synaptic partners (dual-eGRASP) enables specific labelling of activated dendrites and
94 synapses[2]. Dual-eGRASP utilises split protein reconstitution in the synaptic cleft to label
95 synapses. Using two colours of split protein and fluorescence expression, all connection types
96 between engrams (E) and non-engrams (N) can be fluorescently labelled (Fig. 1A-C, S3A).
97 Using this dual-eGRASP technique, synaptic strengthening was quantified in the vCA1-BA
98 circuit after CFC (Fig. 1B, S3B). No significant difference in synaptic density was observed
99 between N-N and N-E across all experimental groups while significantly higher density of E-
100 E synapses was observed in the CFC group compared to the E-N synapses (Fig. 1D). This
101 suggests recruitment of synapses between engram neurones during acquisition of associative
102 memory. Subsequently, morphological changes were investigated to confirm structural
103 plasticity in the spines during associative memory formation. Morphological analysis revealed
104 a significant increase in spine head diameter, spine head volume, and spine volume of E-E
105 synapses in the CFC group compared to N-E synapses (Fig. 1E). The context only group
106 exhibited no significant differences in spine head size of E-E synapses. We conclude that fear
107 conditioning induced structural plasticity specifically in E-E synapses. No significant
108 difference was found in any of the four metrics of structural plasticity between N-N and N-E
109 synapse in the three behavioural groups (Fig. S3F). Consequently, these results indicate that

110 engram synapses undergo structural plasticity during associative fear learning in the vCA1-BA
111 circuit.
112
113 ***De novo* protein quantification using NCAA labelling**
114 A key aspect of memory consolidation theory suggests that *de novo* protein synthesis is
115 essential for synaptic plasticity[21,22]. The use of PSIs has been crucial in advancing this theory,
116 as numerous studies have demonstrated that administering PSIs during memory acquisition
117 impairs natural recall in mice[16]. Therefore, as an indirect method to inhibit synaptic changes
118 observed in Fig 1, we established behavioral conditions for PSI treatment with greater
119 specificity.
120
121 First, to establish experimental conditions for extensive protein synthesis inhibition,
122 noncanonical amino acids (NCAA) labelling using biorthogonal noncanonical amino acid
123 tagging (BONCAT)[23–25] was performed as mice were injected with PSI. Given that the reported
124 time window for memory consolidation extends up to 6 hours after the event[26], initial approach
125 aimed to extend the duration of the PSI treatment[27–29]. It has been previously reported using an
126 electrophysiological approach that four consecutive injections of anisomycin weaken E-E
127 synaptic strengthening[7]. Therefore, mice received four consecutive anisomycin injections
128 (4xANI), or a single anisomycin injection followed by three consecutive saline injections
129 (1xANI), or 4 consecutive saline injections (SAL). Immediately after the CFC, mice were
130 intraperitoneally injected with L-methionine analog L-azidohomoalanine (AHA) which tags
131 newly synthesizing proteins and brains were snap frozen 16 hours after CFC (Fig. 2A).
132 Quantification of NCAA labelled proteins by western blotting showed that 4xANI mice
133 displayed protein intensity comparable to that of AHA(-) mice (Fig. 2B, C). These results
134 suggest that 4xANI injections effectively suppresses protein synthesis.

135

136 **Multiple injections and cocktail of drugs induce retrograde amnesia more effectively**

137 Building on NCAA studies, robust protein synthesis inhibition conditions were applied *in vivo*.
138 For multiple injections, four consecutive injections of saline or anisomycin were delivered (Fig.
139 2A, D). In another experimental condition, a stronger inhibition was achieved with a single
140 injection by using cycloheximide along with anisomycin to inhibit two different ribosomal sites
141 (Fig. S5). In line with the previous study, a single injection of anisomycin decreased natural
142 recall of fear memory[16], while multiple injections of anisomycin and the cocktail group (CKT)
143 exhibited significantly lower freezing levels compared to the single injected group (Fig. 2E,
144 2H, S5A-B). Therefore, these data confirm that extensive protein synthesis inhibition by
145 multiple injections of anisomycin or a cocktail of protein synthesis inhibitors significantly
146 impairs natural recall of fear memory.

147

148 To test whether the memory impairment by injection of PSI leads to impaired engram
149 reactivation, Arc-CreERT2 crossed with floxed tdTomato mice were fear conditioned followed
150 by 4-OHT and a series of PSI injections (Fig. 2D). Immunohistochemistry analysis showed no
151 significant difference in the ratio of tdTomato^{+} or c-Fos^{+} neurones in all three groups (Fig. S4).
152 However, the reactivation ratio between activated neurones during the conditioning and
153 memory recall was significantly lower in the 4xANI group in both vCA1 and BA (Fig. 2I, J).
154 Significant differences in reactivation ratio between groups were replicated using Arc-
155 CreERT2 mice expressing CaMKII-DIO-tdTomato (Fig. 2F, G). Moreover, the single injection
156 of the cocktail significantly reduced the reactivation ratio in the BA compared to treatment
157 with anisomycin alone (Fig. S5). Taken together, these data suggest that multiple injections of
158 anisomycin significantly disrupt the reactivation of engram cells and impair memory recall.

159

160 We next examined whether amnesic memory can be recalled using optogenetics. To reactivate
161 neurones specifically activated during the CFC under different PSI treatments, EF1a-DIO-
162 ChR2-eYFP was bilaterally expressed in the vCA1 of Arc-CreERT2 mice (Fig. 3B, S6A). To
163 reach sufficient virus expression in axon terminals in the BA, mice were tested five days after
164 the CFC (Fig. S6B, C). Restoration of memory from amnesia has been observed by directly
165 stimulating anisomycin-treated DG engram cells with light; this preferential, protein synthesis-
166 independent functional engram connectivity was observed even eight days after the initial
167 training[30]. All groups of mice reported here showed robust freezing acquisition (Fig. 3A). Five
168 days after training, mice were introduced to a novel environment for blue light stimulation. In
169 line with prior research, neither group displayed freezing behaviour when the blue light was
170 off, but SAL groups and 1xANI groups exhibited a significant increase in freezing behaviour
171 when the blue light was on (Fig. 3C-D, S7C-D). Notably, in the CKT and 4xANI group, mice
172 did not display any freezing level during the light on and off sessions (Fig. 3E, Fig. S7E). To
173 assess the conditioned response to recall cues, mice were once more evaluated in the fear-
174 conditioned chamber 24 hours after the optical stimulation. Consistent with our previous data,
175 SAL mice showed robust freezing while 4xANI showed minimal freezing behaviour (Fig. 3B).
176
177 The saline group displayed robust freezing behaviour, whereas the anisomycin group with
178 single injection resulted in significantly reduced freezing behaviour during cued recall (Fig.
179 S7B). The 4xANI and CKT groups exhibited a freezing level similar to naïve mice. These data
180 indicate that the connectivity of vCA1 engram cells to the downstream BA is enhanced during
181 memory acquisition only if the protein synthesis blockade is not extensive, while an extensive
182 blockade inhibits synaptic strengthening between the regions, thus impairing memory.
183

184 Collectively, these data provide evidence supporting the critical role of engram synapses in
185 associative memory by indirectly modulating engram synapse potentiation by multiple PSI
186 injections.
187
188 To investigate the synaptic changes associated with memory under extensive protein synthesis
189 blockade, we applied the dual-eGRASP technique (Fig. 1A). Mice underwent CFC followed
190 by serial injections of either anisomycin or saline (Fig. 4A). Consistent with our previous
191 findings, the group that received four injections of anisomycin (4xANI) exhibited significantly
192 impaired fear memory retrieval compared to the SAL group (Figs. 3B and 4B). Dual-eGRASP
193 analysis revealed an increased density of E-E synapses across all behavioural groups, while no
194 significant differences were observed in N-E synapse density (Figs. 1D and 4C). However, a
195 notable reduction in E-E synapse density was observed in the 4xANI group compared to the
196 1xANI, with no significant difference between the SAL and 1xANI groups (Fig. 4C). This
197 reduction in E-E synapse density may explain the failure of optogenetic reactivation observed
198 in the 4xANI group (Fig. 3E). Additionally, spine morphology analysis revealed increases in
199 spine head diameter, spine head volume, and overall spine volume in the E-E synapses of the
200 SAL group (Figs. 1E and 4D, E). Interestingly, these metrics showed no significant changes in
201 the 1xANI or 4xANI groups, with spine dimensions in the 1xANI group being significantly
202 smaller than those in the SAL group. These findings suggest that the reduction in spine
203 dimensions correlates with impaired natural memory recall observed in the 1xANI group (Fig.
204 3D).
205

206 ## Discussion

207 It has been challenging to determine whether memory formation strengthens the synapses
208 between engram cells in interconnected brain regions[31]. This challenge stems from the

209 difficulty in distinguishing presynaptic regions formed by engram cells from those formed by
210 non-engram cells. The modification of the GRASP technique has provided the solution
211 enabling the visualisation and analysis of spine density and morphology[2]. Additionally, the
212 position of the colour-determining domain in the presynaptic neurone (cyan/yellow pre-
213 eGRASP) and the common domain in the postsynaptic neurone (post-eGRASP), allowed us to
214 visualize two synaptic populations originating from two functionally distinct presynaptic
215 neuronal populations: one involved in encoding the engram and the other not, both projecting
216 onto a single postsynaptic neurone[2].
217
218 Using the dual-eGRASP technique, we investigate the hypothesis that contextual fear learning
219 is associated with the enhancement of synapses between engram cells, the so-called synaptic
220 engram hypothesis[32]. Engram synapses have been shown to be critical in memory acquisition
221 and extinction where changes in engram synapse density and spine head size were observed[2,3].
222 Our results showed similar lines of data, where increased synapse density, spine head size,
223 spine volume, and spine head volume were observed specifically in E-E synapses of vCA1-BA
224 circuit (Fig. 1D, E). Therefore, these data suggest that the engram synapse hypothesis can also
225 be applied to the vCA1-BA circuit during associative fear learning.
226
227 Along with the CFC group, the context only group also exhibited an increase in E-E synaptic
228 density (Fig. 1D). This data is consistent with our previous findings within the CA3-CA1
229 pathway, where the context only group demonstrated significant synaptic changes[2]. This
230 increase in synaptic density may be attributed to Hebbian plasticity between vCA1 engram
231 neurones and BA neurones activated by emotions other than fear, such as anxiety, generated
232 during exposure to the novel context[33] as BA is also known to mediate anxiogenic behaviour[20].

233 Unlike synaptic activity of the vCA1 region drives the increase in synaptic density, although it
234 is not sufficiently pronounced to increase spine size.
235
236 Moreover, to validate the hypothesis that modification of E-E synaptic connectivity is
237 necessary for memory acquisition, we administered PSI to induce retrograde amnesia. In this
238 study, we set optimal conditions for inducing extensive retrograde amnesia by extending the
239 time window of protein synthesis inhibition or simultaneously targeting two ribosomal sites.
240 These experimental conditions induce a more pronounced effectiveness in impairing memory
241 recall.
242
243 It has been reported that a memory that is impaired by inhibiting synaptic potentiation using
244 PSI can later be artificially reactivated[16]. Another study has demonstrated that inhibiting
245 protein synthesis, coupled with the induction of autophagy, results in irretrievable memory[18].
246 To assess whether varying degrees of protein synthesis inhibition produce different behavioural
247 outcomes, we tested multiple groups to identify the optimal condition for inducing memory
248 impairment. This approach led to the discovery that when mice undergo an extensive inhibition
249 of protein synthesis, optogenetic reactivation of engram cells can no longer induce memory
250 recall. Multiple injections of anisomycin showed no significant changes to the number of
251 engram cells (Fig. S4D). Also, E-E synapses showed increased density and enlarged structural
252 morphology during associative fear learning (Fig. 1D, E). Therefore, we propose that the failure
253 of optogenetic reactivation in mice subjected to multiple anisomycin injections is attributed to
254 a reduction in E-E synaptic density caused by extensive protein synthesis inhibition (Fig. 4B).
255 On the other hand, we suggest that the impaired natural recall observed in both 1xANI and
256 4xANI groups is driven by the lack of engram synapse enlargement (Fig.4C). Numerous studies
257 have provided evidence that neither single nor multiple injections of anisomycin are sufficient

258 to block synaptic plasticity to a level comparable to the naïve group[7,16]. Although the
259 AMPAR/NMDAR ratio was lower, EPSC frequency remained elevated, suggesting that
260 synaptic strength weakened while E-E synaptic connections increased[7]. We can conclude that
261 our experimental conditions were sufficient to impair memory recall in both natural and
262 optogenetic reactivation contexts (Fig. 3, 4). However, the residual freezing behaviour and the
263 observed increase in engram synapse density needs further investigation which may be
264 regulated by protein synthesis independent mechanisms such as remodelling of actin skeleton.
265
266 Limitations of the current study arise from the fact that anisomycin affects protein synthesis in
267 a non-discriminatory way. Anisomycin was given by intraperitoneal injection, thereby
268 affecting the whole mouse body. To rule out the possibility that protein synthesis blockade
269 from other regions has contributed to the failure of memory storage, future studies should block
270 protein synthesis in a brain region-specific and engram-specific manner, possibly through the
271 use of genetically encodable PSI[34].
272

273 # References

274 1. Josselyn, S. A., Köhler, S. & Frankland, P. W. Finding the engram. *Nat. Rev.*
275 *Neurosci. 2015 169* **16**, 521–534 (2015).
276 2. Choi, J. H. *et al.* Interregional synaptic maps among engram cells underlie memory
277 formation. *Science (80-.).* **360**, 430–435 (2018).
278 3. Choi, D. Il *et al.* Synaptic correlates of associative fear memory in the lateral
279 amygdala. *Neuron* **109**, 2717-2726.e3 (2021).
280 4. Lee, C. *et al.* Hippocampal engram networks for fear memory recruit new synapses
281 and modify pre-existing synapses in vivo. *Curr. Biol.* **33**, 507-516.e3 (2023).
282 5. Kim, Y., Hong, I. & Kaang, B. K. Synaptic correlates of the corticocortical circuit in

283 motor learning. *Philos. Trans. R. Soc. Lond. B. Biol. Sci.* **379**, (2024).
284 6. Jimenez, J. C. *et al.* Contextual fear memory retrieval by correlated ensembles of
285 ventral CA1 neurons. *Nat. Commun. 2020 111* **11**, 1–11 (2020).
286 7. Kim, W. Bin & Cho, J. H. Encoding of contextual fear memory in hippocampal–
287 amygdala circuit. *Nat. Commun.* **11**, 1–22 (2020).
288 8. Hong, I. & Kaang, B. K. The complexity of ventral CA1 and its multiple
289 functionalities. *Genes. Brain. Behav.* **21**, (2022).
290 9. Nonaka, A. *et al.* Synaptic plasticity associated with a memory engram in the
291 basolateral amygdala. *J. Neurosci.* **34**, 9305–9309 (2014).
292 10. Teng, S. W. *et al.* Altered fear engram encoding underlying conditioned versus
293 unconditioned stimulus-initiated memory updating. *Sci. Adv.* **9**, 1–17 (2023).
294 11. Kang, H. & Schuman, E. M. A requirement for local protein synthesis in neurotrophin-
295 induced hippocampal synaptic plasticity. *Science (80-.).* **273**, 1402–1406 (1996).
296 12. Sun, C. *et al.* The prevalence and specificity of local protein synthesis during neuronal
297 synaptic plasticity. *Sci. Adv.* **7**, 790–807 (2021).
298 13. Schafe, G. E. *et al.* Activation of ERK/MAP kinase in the amygdala is required for
299 memory consolidation of pavlovian fear conditioning. *J. Neurosci.* **20**, 8177–8187
300 (2000).
301 14. Schafe, G. E. & LeDoux, J. E. Memory consolidation of auditory pavlovian fear
302 conditioning requires protein synthesis and protein kinase A in the amygdala. *J.*
303 *Neurosci.* **20**, (2000).
304 15. Fonseca, R., Vabulas, R. M., Hartl, F. U., Bonhoeffer, T. & Nägerl, U. V. A balance of
305 protein synthesis and proteasome-dependent degradation determines the maintenance
306 of LTP. *Neuron* **52**, 239–245 (2006).
307 16. Ryan, T. J., Roy, D. S., Pignatelli, M., Arons, A. & Tonegawa, S. Engram cells retain

308 memory under retrograde amnesia. *Science (80-.).* **348**, 1007–1013 (2015).

309 17. Roy, D. S. *et al.* Memory retrieval by activating engram cells in mouse models of early
310 Alzheimer's disease. *Nature* **531**, 508–512 (2016).

311 18. Abdou, K. *et al.* Synapse-specific representation of the identity of overlapping memory
312 engrams. *Science (80-.).* **360**, 1227–1231 (2018).

313 19. Gergues, M. M. *et al.* Circuit and molecular architecture of a ventral hippocampal
314 network. *Nat. Neurosci.* **23**, 1444–1452 (2020).

315 20. Pi, G. *et al.* Posterior basolateral amygdala to ventral hippocampal CA1 drives
316 approach behaviour to exert an anxiolytic effect. *Nat. Commun.* **11**, (2020).

317 21. Kandel, E. R. The molecular biology of memory storage: a dialogue between genes
318 and synapses. *Science* **294**, 1030–1038 (2001).

319 22. Costa-Mattioli, M., Sossin, W. S., Klann, E. & Sonenberg, N. Translational control of
320 long-lasting synaptic plasticity and memory. *Neuron* **61**, 10–26 (2009).

321 23. Dieterich, D. C., Link, A. J., Graumann, J., Tirrell, D. A. & Schuman, E. M. Selective
322 identification of newly synthesized proteins in mammalian cells using bioorthogonal
323 noncanonical amino acid tagging (BONCAT). *Proc. Natl. Acad. Sci. U. S. A.* **103**,
324 9482–9487 (2006).

325 24. Dieterich, D. C. *et al.* Labeling, detection and identification of newly synthesized
326 proteomes with bioorthogonal non-canonical amino-acid tagging. *Nat. Protoc.* **2**, 532–
327 540 (2007).

328 25. Dieterich, D. C. *et al.* In situ visualization and dynamics of newly synthesized proteins
329 in rat hippocampal neurons. *Nat. Neurosci.* **13**, 897–905 (2010).

330 26. Casagrande, M. A. *et al.* Synaptic consolidation as a temporally variable process:
331 Uncovering the parameters modulating its time-course. *Neurobiol. Learn. Mem.* **150**,
332 42–47 (2018).

333 27. Squire, L. R., Kuczenski, R. & Barondes, S. H. Tyrosine hydroxylase inhibition by
334 cycloheximide and anisomycin is not responsible for their amnesic effect. *Brain Res.*
335 **82**, 241–248 (1974).
336 28. Flood, J. F., Bennett, E. L., Orme, A. E., Rosenzweig, M. R. & Jarvik, M. E. Memory:
337 Modification of anisomycin-induced amnesia by stimulants and depressants. *Science*
338 *(80-.).* **199**, 324–326 (1978).
339 29. Freeman, F. M., Rose, S. P. R. & Scholey, A. B. Two Time Windows of Anisomycin-
340 Induced Amnesia for Passive Avoidance Training in the Day-Old Chick. *Neurobiol.*
341 *Learn. Mem.* **63**, 291–295 (1995).
342 30. Roy, D. S., Muralidhar, S., Smith, L. M. & Tonegawa, S. Silent memory engrams as
343 the basis for retrograde amnesia. *Proc. Natl. Acad. Sci. U. S. A.* **114**, E9972–E9979
344 (2017).
345 31. Hebb, D. 0. The Organization of Behavior A NEUROPSYCHOLOGICAL THEORY.
346 (1949).
347 32. Han, D. H., Park, P., Choi, D. Il, Bliss, T. V. P. & Kaang, B. K. The essence of the
348 engram: Cellular or synaptic? *Seminars in Cell and Developmental Biology* (2021)
349 doi:10.1016/j.semcdb.2021.05.033.
350 33. Tye, K. M. *et al.* Amygdala circuitry mediating reversible and bidirectional control of
351 anxiety. *Nature* **471**, 358–362 (2011).
352 34. Heumüller, M., Glock, C., Rangaraju, V., Biever, A. & Schuman, E. M. A genetically
353 encodable cell-type-specific protein synthesis inhibitor. *Nat. Methods 2019 168* **16**,
354 699–702 (2019).
355 35. Fripont, S., Marneffe, C., Marino, M., Rincon, M. Y. & Holt, M. G. Production,
356 purification, and quality control for adeno-associated virusbased vectors. *J. Vis. Exp.*
357 **2019**, e58960 (2019).

36. Evans, H. T., Bodea, L. G. & Götz, J. Cell-specific non-canonical amino acid labelling identifies changes in the de novo proteome during memory formation. *Elife* **9**, 1–19 (2020).

Materials and methods

Animals

All experiments were conducted in accordance with the regulations and guidelines of the Institutional Animal Care and Use Committees (IACUC) of Seoul National University. Investigators were not blinded to the genotypes of the mice.

Wild-type C57BL/6N mice were used for dual-eGRASP experiments, while wild-type C57BL/6J mice were used for BONCAT. Heterozygous Arc-CreERT2 (Jackson Laboratory Stock # 022357) mice, obtained by crossing wild-type C57BL6/J and Arc-CreERT2 (+/−) mice, were utilised to label engram neurones and for optogenetic experiments. Heterozygous Arc-CreERT2; Ai14 mice, obtained by crossing Ai14 (Jackson Laboratory Stock # 007914) and Arc-CreERT2 (+/−) mice, were used to label engram neurones in the experiments.

Mice were housed in standard laboratory cages with disposable bedding on a standard light cycle (09h-21h). Mice had access to food and water *ad libitum* and were socially housed in numbers of three to five littermates until surgery. Behavioural experiments were performed during the light cycle. Male and/or female mice were utilised in the experiments with details provided in the figures or figure legends

AAV production

382 Adeno-associated virus serotype 1/2 (AAV1/2; AAV particle containing both serotype 1 and 2
383 capsids) was used for injection as previously described[2].
384
385 The procedure for packaging plasmids into adeno-associated virus serotype 9 (AAV9) involved
386 the following steps: plasmids containing the construct of interest flanked by AAV2 ITR, pAd-
387 ΔF6, and pRep/Cap9 were co-transfected into the AAVpro 293T Cell Line (TAKARA, cat#
388 632273). The transfected cells were then incubated in DMEM with 10% v/v FBS for five days
389 in a 150 mm culture dish. On the day of harvest, culture medium was collected and the
390 remaining cells were lysed to extract any virus they contained. After centrifugation at 13,490
391 g for 60 minutes at 4°C, the supernatants were carefully loaded into ultracentrifugation tubes
392 filled with iodixanol gradient solutions.
393
394 AAV was purified from the cell lysate using iodixanol density-gradient ultracentrifugation as
395 previously described[35]. 40% iodixanol solutions were withdrawn using 5 mL syringes and
396 further concentrated using Amicon Ultra 100-kDa MWCO ultrafiltration centrifugal devices
397 (Merck, cat# UFC910024).
398
399 **Virus-mediated gene expression**
400 For c-Fos labelling experiments, the virus comprised AAV1/2-Fos-rtTA mixed with AAV1/2-
401 TRE-mCherryNuc. Virus was bidirectionally injected into both vCA1 (500 nl; AP: -3.1 mm,
402 ML: ±3.4 mm DV: -3.8 mm) and BA (500 nl; AP: -1.5 mm ML: ±3.0 mm, DV: -4.9 mm).
403
404 AAV9- EF1α-DIO-ChR2-EYFP was acquired from Institute for Basic Science Recombinant
405 Virus Packaging Facility.
406

407 **Stereotaxic surgery procedure**

408 Mice were anaesthetised by intraperitoneal injection of 25 $mg \cdot kg^{-1}$ ketamine/xylazine and
409 positioned on a stereotaxic apparatus (Stoelting Co.). Ophthalmic ointment was applied to the
410 eyes as a preventive measure against dryness. Bilateral craniotomies were performed using a
411 0.5 mm diameter drill and the viruses were injected using a micro-needle attached to a 10 mL
412 Hamilton micro syringe (Hamilton; cat# 701LT). A syringe driver (WPI, cat# SP3101-PLUS)
413 was used to maintain the speed of the injection at 0.125 $ul \cdot min^{-1}$. The needle was slowly
414 lowered to the target site and remained for 2 minutes before beginning the injection. After
415 injection, the needle stayed for 10 minutes before it was slowly withdrawn. The incision was
416 sutured, and mice were allowed to recover for 2 weeks before the start of behavioural
417 experiment.

418

419 For the optogenetic experiment, a custom implant containing two optic fibres (Newdoon; 0.37
420 NA 1.25 mm core diameter) was lowered above the injection site at the following coordinate
421 relative to bregma (mm): AP: -1.5 ML: ±3.0 DV: -4.0 for BA. A jewellery screw was screwed
422 into the skull near the bregma. Mice were allowed to recover for at least 2 weeks before
423 behavioural experiments.

424

425 **Contextual fear conditioning**

426 Two weeks following AAV injection, all mice underwent a conditioning procedure. Prior to
427 conditioning, each mouse was housed individually for eight days and was subjected to daily
428 handling sessions lasting five minutes for seven consecutive days. Mice were randomly
429 assigned to either the CFC group or the context only control group. Mice were transferred from
430 the vivarium to a holding room adjacent to the testing area at least 30 minutes prior to the start

431 of the experiment. Furthermore, each mouse was transported individually to the conditioning
432 room.
433
434 The conditioning chamber measuring 7”W × 7”D × 12”H (Coulbourn Instruments; model H10-
435 11M-TC) was used. The chamber featured two aluminium side walls and a ceiling with an
436 acrylic door. It was situated within a larger sound-attenuating enclosure. Throughout the
437 experimental procedures, a white overhead light continuously illuminated the conditioning
438 chamber. The chamber itself was equipped with a straight stainless-steel rod floor which was
439 cleaned using a 70% ethanol solution and distilled water between each use.
440
441 Two hours prior to the conditioning procedure, an intraperitoneal injection of 250 µL of a 5
442 $mg \cdot ml^{-1}$ Doxycycline solution dissolved in saline was administered. For contextual fear
443 conditioning, mice were exposed to the context for 180 seconds, after which five-foot shocks
444 were delivered where each foot shock lasted 2 seconds with an interval of 2 minutes. Following
445 the conditioning session, mice were returned to their respective home cages. During the
446 retrieval test, the percentage of time spent freezing was calculated and averaged across the
447 entire 3-minute retrieval session.
448
449 **BONCAT**
450 General procedures for BONCAT was followed as previously described[23–25]. AHA was
451 dissolved in PBS (NaCl 137 mM, KCl 2.7 mM, Na_2HPO_4 4.3 mM, KH_2PO_4 1.47 mM) and
452 administered via intraperitoneal injection. The labelling duration was set as 16 hours following
453 the established treatment protocol for optimal results[36] with a dosage of 100 µg $NCAA \cdot gbw^{-1}$
454 (gram body weight). After the designated treatment period, mice were deeply anesthetised with
455 isoflurane followed by brain removal. The vCA1 and BA were sliced in the artificial

456 cerebrospinal fluid (NaCl 124 mM, KCl 3 mM, $NaHCO_3$ 26 mM, NaH2PO_4 1.25 mM, $MgSO_4$
457 2 mM, D-glucose 15 mM, $CaCl_2$ 2 mM) carbonated with 95% O_2 and 5% CO_2 into 300µm
458 sections using a vibratome (Leica; VT1200S). Brains were dissected under a dissecting
459 microscope and frozen using liquid nitrogen.
460
461 To create working stocks of 4-Hydroxytamoxifen (4-OHT) at a concentration of 20 $mg \cdot ml^{-1}$,
462 50 mg of 4-OHT (Sigma Aldrich, cat# H6278) were dissolved in 2.5 ml of 100% ethanol. These
463 working stocks of 4-OHT were stored at -20°C for a maximum of three months. On the day of
464 use, working stocks were further diluted with a mixture of castor oil and sunflower oil at a 1:4
465 ratio (Sigma Aldrich, cat# 259853 and cat# S5007) via vacuum centrifugation resulting in a
466 final concentration of 10 mg·ml-1.
467
468 Anisomycin (Tocris, cat# 1290) and cycloheximide (Sigma Aldrich, cat# 239763-M) were
469 stored at -20°C up to a year, and the powder was dissolved with saline on the day of use.
470
471 **BONCAT purification and Immunoblotting**
472 General procedures for BONCAT was followed as previously described[23–25]. The protein
473 concentration was assessed using a Pierce BCA protein assay kit (Thermo Fisher Scientific)
474 following the manufacturer's guidelines. Subsequently, an equal volume of protein samples
475 was subjected to electrophoresis on a 4 to 12% gradient gel (BIO-RAD, cat#4561084) and
476 transferred onto a PVDF membrane (Invitrogen, cat#IB24001). The membranes were blocked
477 using 4% bovine serum albumin in Tris-Buffered Saline, 0.1% Tween® 20 (TBST) and then
478 incubated with anti-Biotin (1:1000, cat#5597, Cell Signalling) overnight at 4°C. Blots were
479 washed three times in TBST and then incubated with the secondary antibody (anti-rabbit HRP,
480 1:5000, Invitrogen; cat#Q-11071MP) at room temperature for 2 hours. The bands were

481 visualised utilising a West-Q Chemiluminescent Substrate Kit (GenDEPOT, W3651-012) and
482 the ChemiDoc XRS+ system (Bio-Rad; cat#721BR02655). Signal detection and quantification
483 were performed using the ChemiDoc MP device (Bio-Rad).
484
485 **Optogenetics**
486 For the single injection groups, mice were either injected with saline, anisomycin, or
487 anisomycin + cycloheximide right after conditioning. For the multiple injection groups, mice
488 were first injected with saline or anisomycin, followed by three injections with saline or
489 anisomycin at 2 hours of intervals. 4-OHT was injected intraperitoneally for 50 $mg \cdot kg^{-1}$10
490 minutes after the first injection. For the immunohistochemistry, mice were retrieved two days
491 after the conditioning and perfused 90 minutes after retrieval. For optogenetics, mice were
492 habituated to optical cables for at least 30 minutes before the experiment. From 30 to 60
493 minutes of habituation, mice were placed in the acrylic chamber. Mice were allowed to freely
494 move within the acrylic chamber and freezing behaviour was recorded for 8 minutes, with 2
495 minutes of two consecutive lights 'off' and 'on' sessions.
496
497 **Immunohistochemistry**
498 90 minutes after retrieval, mice were deeply anesthetised using ketamine/xylazine (15 $mg \cdot kg^{-}$
499 ^{1}) followed by transcranial perfusion with 15 ml of PBS and 15 ml of 4% PFA. Brains were
500 removed, post-fixed overnight at 4°C in 4% PFA and dehydrated in a 30% sucrose solution in
501 PBS at 4°C for two days. The brain was rinsed with PBS and subsequently frozen at -80°C for
502 a minimum of one hour. Coronal sectioning was performed using a cryostat (Leica) with a
503 thickness of 30 µm. The sections were rinsed with 1 mL of PBS for 5 minutes each time at
504 room temperature (RT), 120 rpm. Then 500 µL of a blocking solution (5% normal goat serum,
505 0.3% triton X-100 in PBS) was applied to each sample for 1hr RT, 80 rpm. The primary c-Fos

506 antibody (SySy, cat# 226 003) was applied at a concentration of 1:1000 for 24 hours on a
507 shaker at 4 °C. Sections were washed three times with PBS for 5 minutes each time at room
508 temperature (RT), 120 rpm. A secondary antibody (Alexa-488; 1:500) was applied at a
509 concentration of 1:500 for 2 hours at 80 rpm. Finally, sections were washed with 1 mL of PBS
510 three times for 5 minutes each time at 120 rpm, RT. The second washing step included DAPI
511 staining at a concentration of 1:1000 for 5 minutes at 80 rpm, RT. Cell counting was manually
512 performed using Imaris (Bitplane) by an experimenter who was blinded to the conditions.
513
514 **Confocal imaging**
515 10-15 z-stacks per animal were taken for the immunohistochemistry analysis. Around 50-100
516 z-stacks were taken for the dual-eGRASP density analysis, while 30-50 z-stacks of the image
517 were used to analyse synaptic morphology. All samples were imaged using Leica SP8 confocal
518 microscope or Leica Stellaris 5 with 63x objective with distilled water immersion and 10x
519 objective lens was used for the immunohistochemistry. Images were taken within −2.9 to −3.8
520 mm bregma, spanning a range of ventral CA1 and -1.3 to 1.8 mm bregma for the BA.
521
522 Each dendrite expressing mScarlet-I or iRFP670 was identified and manually labelled as a
523 filament using a filament tracer in IMARIS. To eliminate bias, other fluorescent signals were
524 concealed. Cyan or yellow eGRASP signals were automatically detected and marked as cyan
525 or yellow spheres. An overlap between cyan and yellow eGRASP signals was considered a
526 yellow signal as it indicated that the presynaptic neurone of the synapse was c-Fos+ during
527 memory formation. Dendrites lacking cyan or yellow eGRASP signals were excluded from
528 further detailed analysis.
529

530 Spines on the designated mScarlet-I+ and iRFP670+ dendrites were manually reconstructed,
531 and their diameter and volume were automatically detected. Each spine was categorised as
532 either an activated spine or a non-activated spine based on the presence of a yellow or cyan
533 eGRASP signal, determined through manual inspection. Measurements of spine head diameter,
534 spine head volume, and spine length were performed using Imaris Filament Tracer. Importantly,
535 the examiner conducting the spine 3D model reconstructions was kept blind to any eGRASP
536 signals to prevent bias. Normalisation of the raw data was performed on a per-image basis to
537 measure synaptic density and on a per-dendrite basis for morphology analysis. For the iRFP
538 dendrite (for density analysis) or cyan-only spine morphology, the raw values were averaged,
539 and then the raw values of each cyan-only spine and yellow spine were divided by this average.
540 The resulting normalised values were utilised for subsequent statistical analysis.
541
542 **Statistical analysis**
543 Data analysis was performed on Prism (GraphPad Software). The α value was set at 0.05 for
544 all analyses.

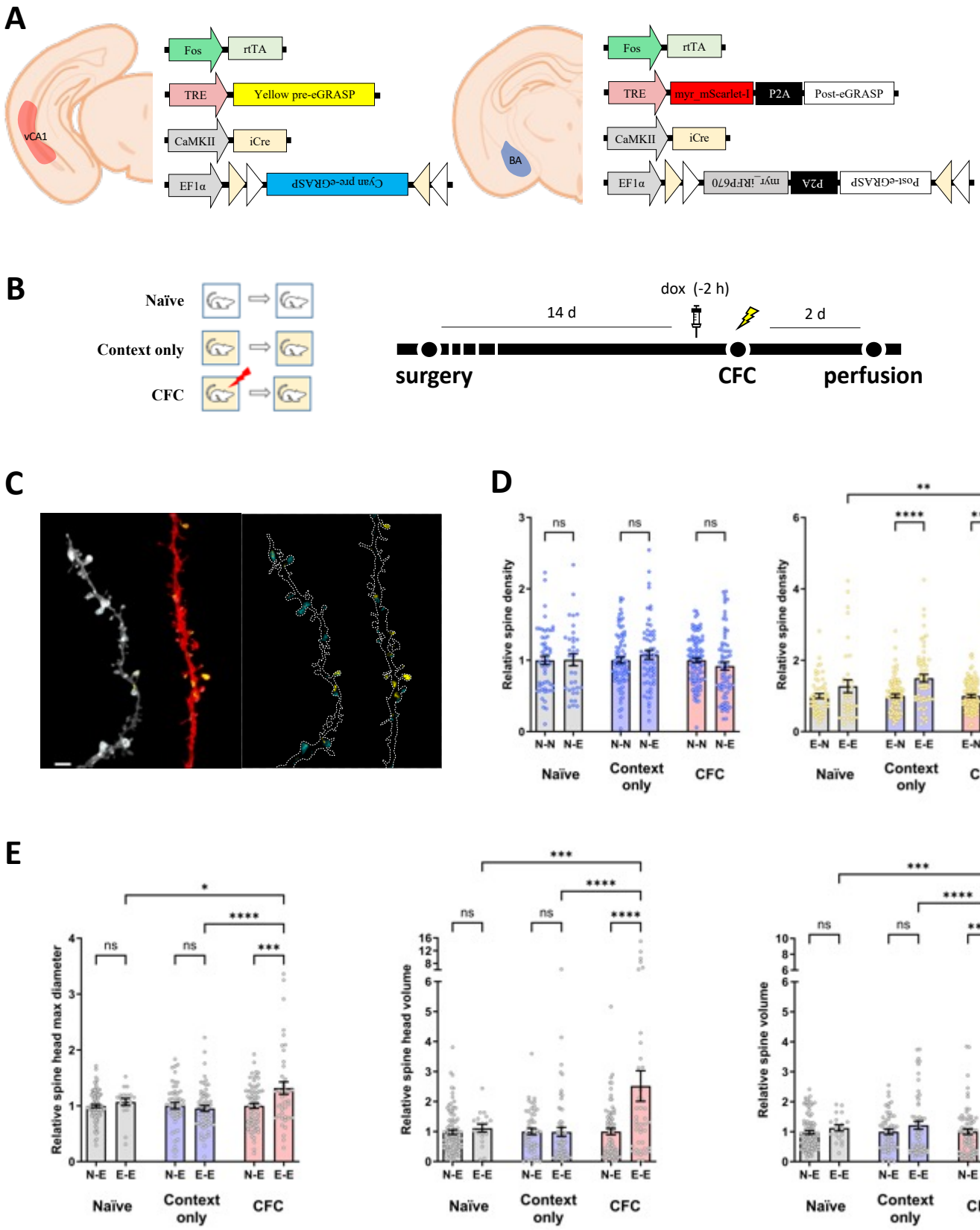
A
vCA1
Fos
rtTA
TRE
Yellow pre-eGRASP
CaMKII
iCre
EF1α
Cyan pre-eGRASP
BA
Fos
rtTA
TRE
myr_mScarlet-I
P2A
Post-eGRASP
CaMKII
iCre
EF1α
Post-eGRASP
P2A
myr_iRFP670
B
Naïve
Context only
CFC
dox (-2 h)
14 d
2 d
surgery
CFC
perfusion
C
D
Relative spine density
ns
N-N
N-E
E-N
E-E
Naïve
Context only
CFC
**
****
E
Relative spine head max diameter
Relative spine head volume
Relative spine volume
*
***

Figure 1. Synaptic density between the vCA1-BA pathway

(**A**) Illustration of virus injection sites. Injection in each site was performed with a cocktail of all the viruses shown for each site.

(**B**) Schematic of the experimental protocol.

(**C**) Illustrative image depicts both engram (red) and nonengram (gray) dendrites with dual-eGRASP labelling in the BA. Cyan signals represent random vCA1 inputs while yellow signals indicate vCA1 engram inputs. Scale bar : 3 μm

(**D**) Normalised cyan/yellow eGRASP per dendritic length. The densities of cyan-only or yellow puncta on mScarlet-I^{+} dendrites are normalised to the corresponding cyan-only or yellow puncta on iRFP670^{+} dendrites from the same images to exclude the effect of different number of vCA1 cells expressing each presynaptic component. Each data point represents a dendrite. Naïve group, n = 45 for BA non engram dendrites, n = 27 for BA engram dendrites; Context only group, n = 106 for BA non engram dendrites; n = 66 for BA engram dendrites; CFC group, n = 73 for BA non engram dendrites; n = 62 for BA engram dendrites. Two-way ANOVA followed by Tukey's multiple comparison test. **P = 0.0063; ****P < 0.0001. Data are presented as mean ± SEM.

(**E**) Normalised spine head diameters, spine head volume and spine volume of dendrites from BA engram cells. Naïve group N-E, n = 111; E-E, n = 32; Context only group N-E, n = 107; E-E, n = 75; CFC group N-E, n = 71; E-E, n = 37. Two-way ANOVA followed by Tukey's multiple comparison test. spine head diameter *P = 0.0315; ***P = 0.0001, spine head volume ***P = 0.0004; ****P < 0.0001, spine volume ***P = 0.0001; ****P < 0.0001. Data are presented as mean ± SEM.

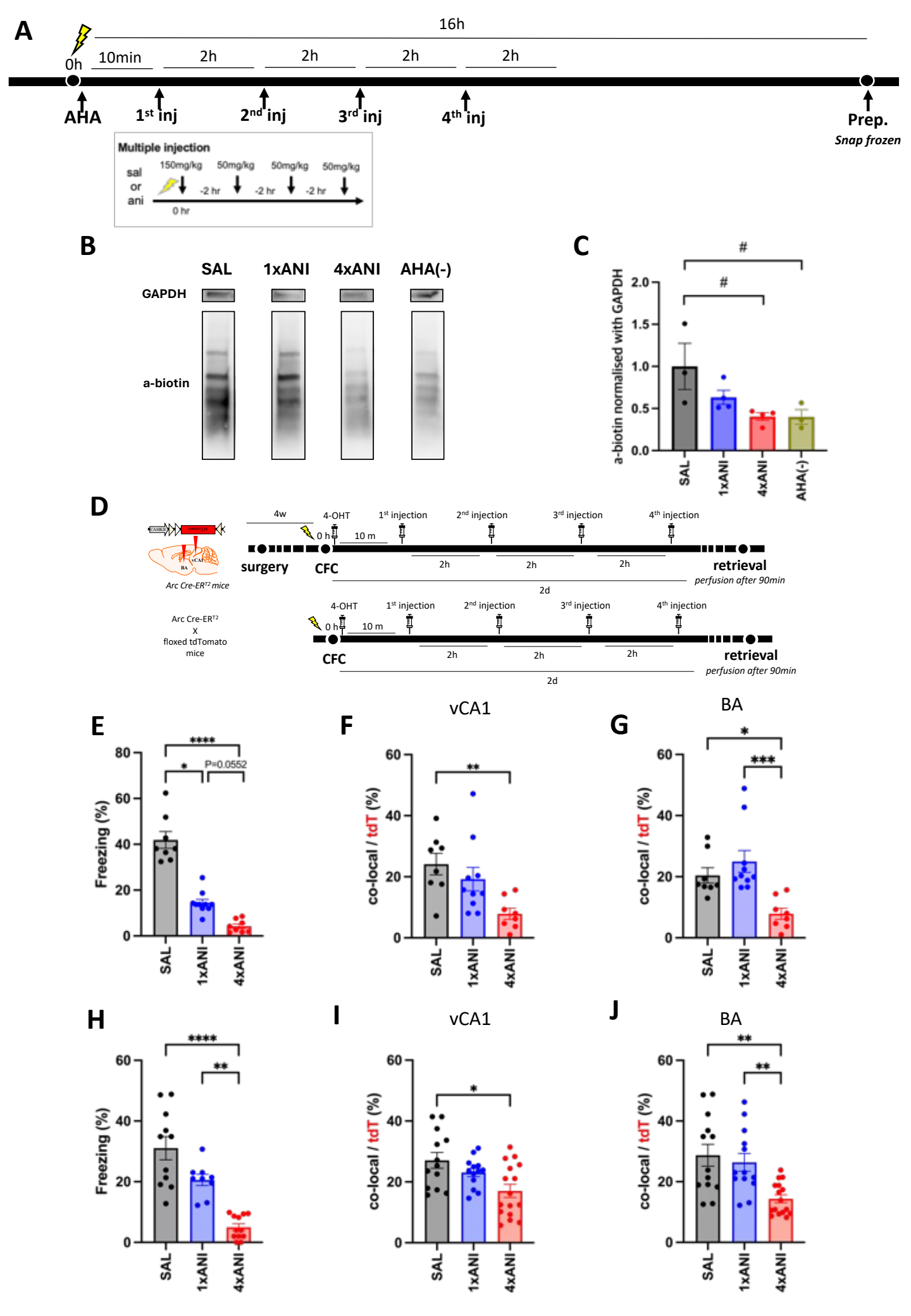
A
16h
0h
10min
2h
2h
2h
2h
AHA
1st inj
2nd inj
3rd inj
4th inj
Prep.
Snap frozen
Multiple injection
sal or ani
150mg/kg
50mg/kg
50mg/kg
50mg/kg
-2 hr
-2 hr
-2 hr
0 hr
B
SAL
1xANI
4xANI
AHA(-)
GAPDH
a-biotin
C
a-biotin normalised with GAPDH
SAL
1xANI
4xANI
AHA(-)
D
4w
4-OHT
1st injection
2nd injection
3rd injection
4th injection
10 m
surgery
CFC
retrieval
perfusion after 90min
2d
Arc Cre-ERT2 mice
Arc Cre-ERT2
X
floxed tdTomato
mice
E
Freezing (%)
P=0.0552
F
vCA1
co-local / tdT (%)
G
BA
co-local / tdT (%)
H
Freezing (%)
I
vCA1
co-local / tdT (%)
J
BA
co-local / tdT (%)

Fig 2. Engram cells are less reactivated by fear recall with multiple anisomycin injections.

(A) Behavioural procedure for NCAA labelling.

(B) Western blot image to tag *de novo* synthesized proteins during memory acquisition

(C) Quantification of the de novo protein synthesis level normalised using GAPDH. SAL group, N = 3; 1xANI group, N = 4; 4xANI group, N = 4; AHA(-) group, N = 3. Kruskal-Wallis test followed by two-stage linear step-up procedure of Bejamini, Kriegar and Yekutieli. #P = 0.0776. Data are presented as mean ± SEM.

(D) Behavioural procedure for testing engram reactivation ratio.

(E-J) Data of engram reactivation analysis for Arc-CreERT2 mice expressing viral CaMKII-DIO-tdTomato (E-G) or crossed with floxed tdTomato (H-J). (E, H) Freezing level during memory recall session. 4xANI group showed lower freezing level compared to that of 1xANI group in both conditions. Engram reactivation ratio of vCA1 neurones (F, I) and BA neurones (G, J). Significantly lower reactivation ratio of BA neurones was observed in 4xANI group compared to 1xANI group. (E-G) SAL group, N = 8; 1xANI group, N = 10; 4xANI group, N = 8. (H-J) SAL group, N = 13; 1xANI group, N = 13; 4xANI group, N = 16. Kruskal-Wallis test followed by Dunn's multiple comparison test. (E) *P = 0.0336; ****P < 0.0001. (F) **P = 0.0045. (G) *P = 0.0148; ***P = 0.0003. (H) ****P < 0.0001; **P = 0.0033. (I) *P = 0.0230. (J) SAL vs. 4xANI, **P = 0.0027; 1xANI vs. 4xANI, **P = 0.0041. Data are presented as mean ± SEM.

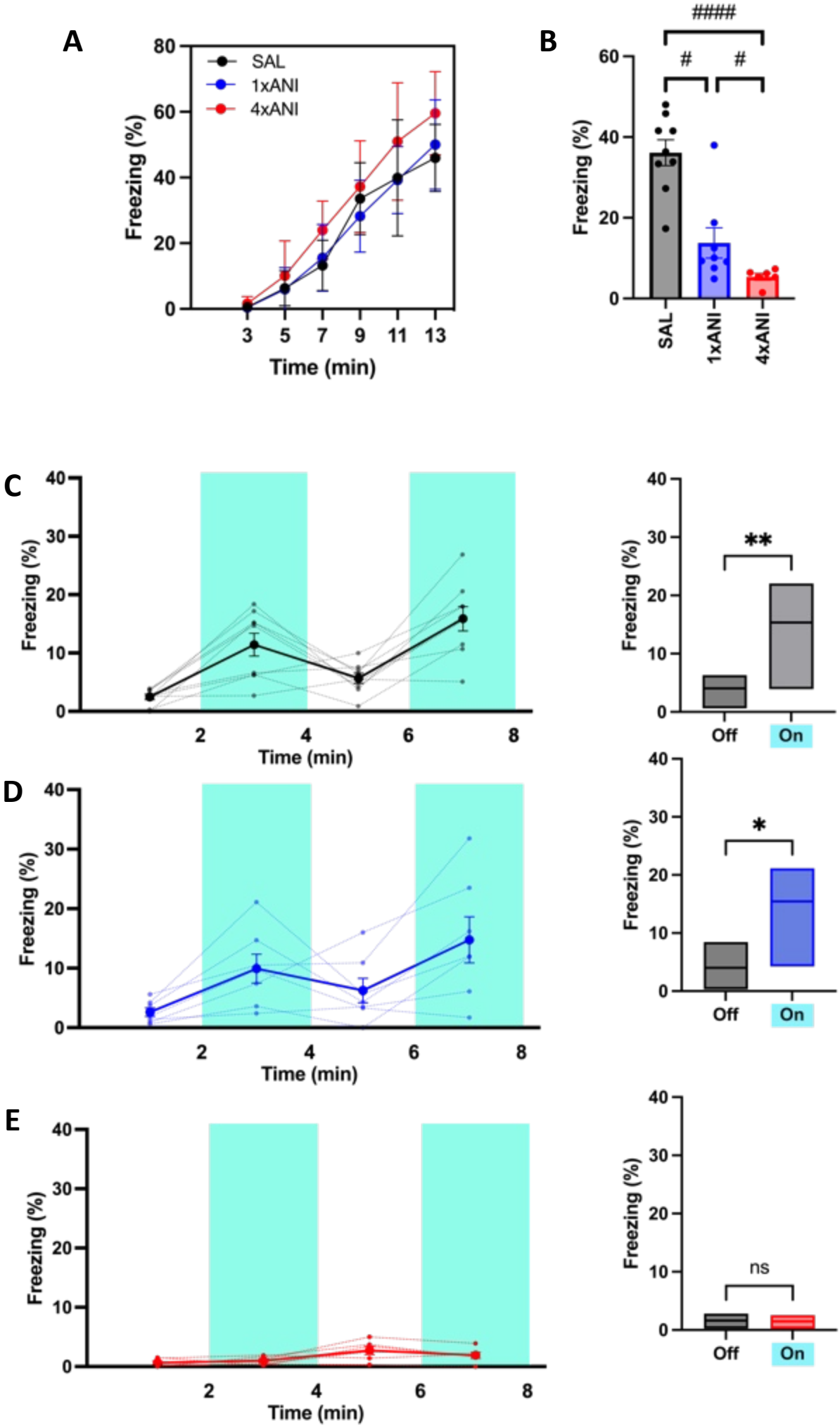
A
SAL
1xANI
4xANI
Freezing (%)
Time (min)
B
#####
#
#
Freezing (%)
SAL
1xANI
4xANI
C
Freezing (%)
Time (min)
**
Off
On
D
Freezing (%)
Time (min)
*
Off
On
E
Freezing (%)
Time (min)
ns
Off
On

Figure 3. Memory cannot be artificially recalled when protein synthesis was blocked for extensive time during memory acquisition.

(A) Freezing level during memory acquisition. Data are presented as mean ± SEM.

(B) Freezing level during contextual fear memory retrieval. SAL group, N = 9; 1xANI group, N = 7; 4xANI group, N = 6. Kruskal-Wallis test followed by two-stage linear step-up procedure of Bejamini, Kriegar and Yekutieli. SAL vs. 1xANI, $^{\#}q = 0.0193$; 1xANI vs. 4xANI, $^{\#}q = 0.0859$; $^{\#\#\#\#}q < 0.0001$. Data are presented as mean ± SEM.

(C-E) Optogenetic activation of vCA1 engram axon terminals in BA of mice treated with PSI during memory acquisition. Mice expressing ChR2 in vCA1 engram cells from CFC show greater freezing during light-on in saline treated control group (C) or by a single treatment of anisomycin (D) while absence of freezing behaviour was shown in mice treated with multiple injection of anisomycin (E). Wilcoxon test. SAL group, **P = 0.0078; 1xANI group, *P = 0.0156. Data are presented as mean ± SEM (left) or median (right).

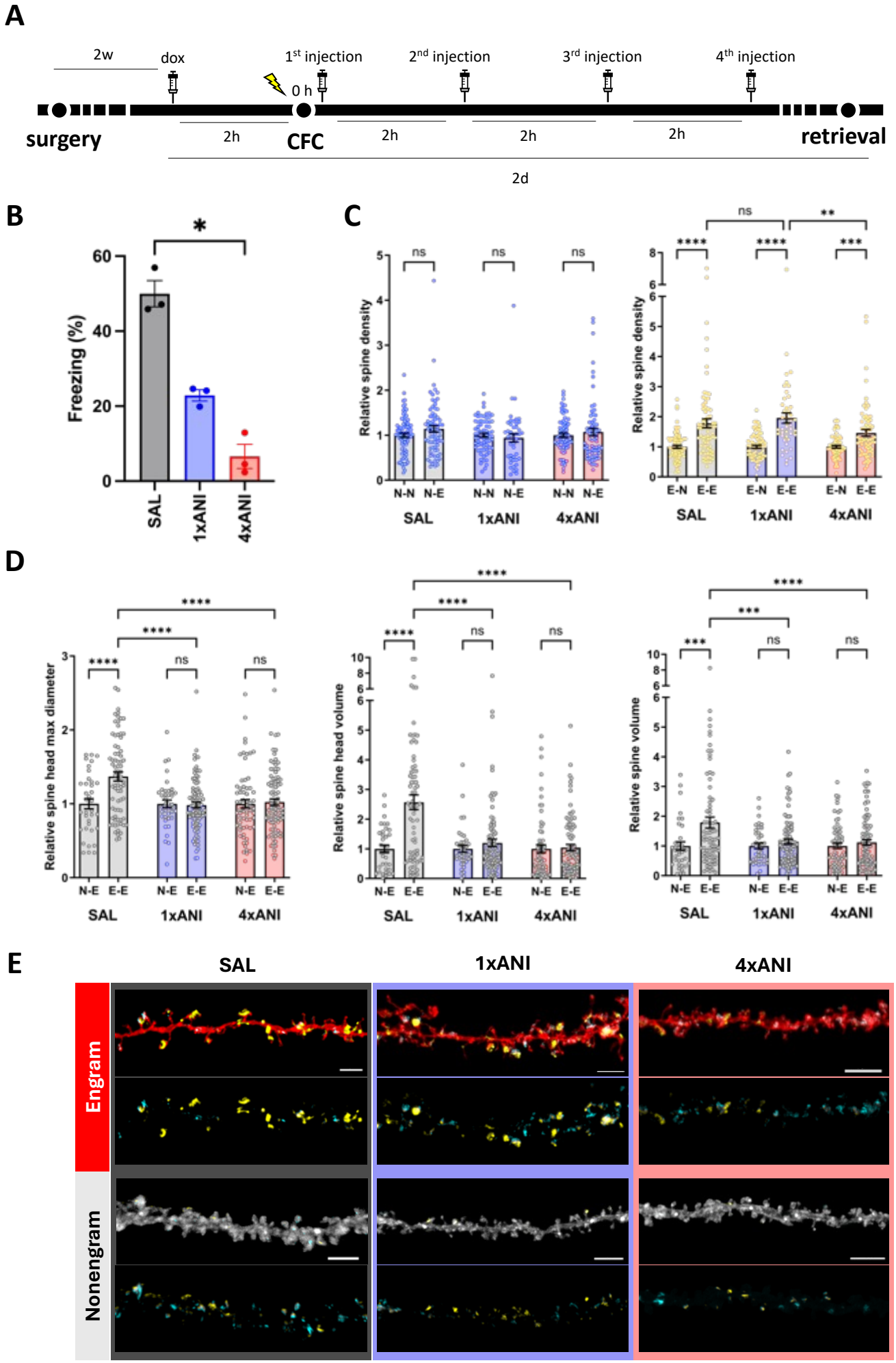
A
2w
dox
1st injection
2nd injection
3rd injection
4th injection
0 h
surgery
2h
CFC
2h
2h
2h
retrieval
2d
B
Freezing (%)
SAL
1xANI
4xANI
C
Relative spine density
N-N
N-E
E-N
E-E
ns
D
Relative spine head max diameter
Relative spine head volume
Relative spine volume
E
SAL
1xANI
4xANI
Engram
Nonengram

Figure 4. Reduced E-E Synapse Density using dual-eGRASP correlates with impaired optogenetic reactivation in 4xANI

(A) Schematic of the behavioural experiment. Mice were intraperitoneally injected with doxycycline 2 hours prior to CFC. After CFC, 4 consecutive anisomycin was intraperitoneally delivered. 2 days following CFC, mice were subjected to fear memory retrieval.

(B) Freezing level during contextual fear memory retrieval for the dual-eGRASP experiment. SAL group, N = 3; 1xANI group, N = 3; 4xANI group, N = 3. Kruskal-Wallis test followed by Dunn's multiple comparison test. *P = 0.0219. Data are presented as mean ± SEM.

(C) Normalised cyan/yellow eGRASP per dendritic length. The densities of cyan-only or yellow puncta on red dendrites are normalised to the corresponding cyan-only or yellow puncta on near-infrared dendrites from the same images to exclude the effect of different number of vCA1 cells expressing each presynaptic component. Each data point represents a dendrite. SAL group, n = 85 for BA nonengram dendrites, n = 74 for BA engram dendrites; 1xANI group, n = 70 for BA nonengram dendrites; n = 45 for BA engram dendrites; 4xANI group, n = 75 for BA nonengram dendrites; n = 69 for BA engram dendrites. Two-way ANOVA followed by Tukey's multiple comparison test. **P = 0.0043; ***P = 0.0008; ****P < 0.0001. Data are presented as mean ± SEM.

(D) Normalised spine head diameter, spine head volume and spine volume of dendrites from BA engram cells. SAL group N-E, n = 36; E-E, n = 76; 1xANI group N-E, n = 39; E-E, n = 93; 4xANI group N-E, n = 66; E-E, n = 93. Two-way ANOVA followed by Turkey's multiple comparison test. spine head diameter ****P < 0.0001, spine head volume ****P < 0.0001, spine volume ***P = 0.0001; ****P < 0.0001. Data are presented as mean ± SEM.

(E) Representative confocal image of both engram and nonengram dendrites from all three behavioural groups. Scale bar : SAL engram, 3 μm; SAL nonengram, 4 μm; 1xANI engram, 4 μm; 1xANI nonengram, 5 μm; 4xANI engram, 5 μm; 4xANI nonengram, 6 μm.

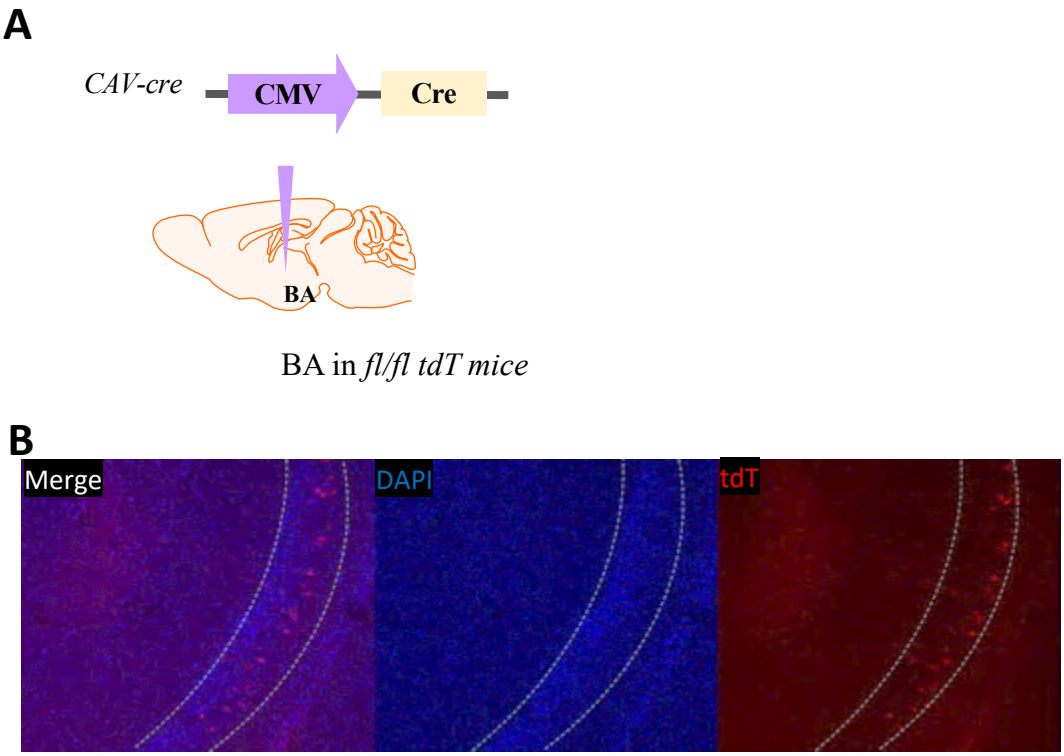

Fig. S1

vCA1 neurones projecting to the BA are mainly residing in the superficial layer

(A) CAV-Cre virus injected into the BA of double floxed tdTomato mice

(B) Images showing BA-projecting vCA1 neurones (tdT^+)

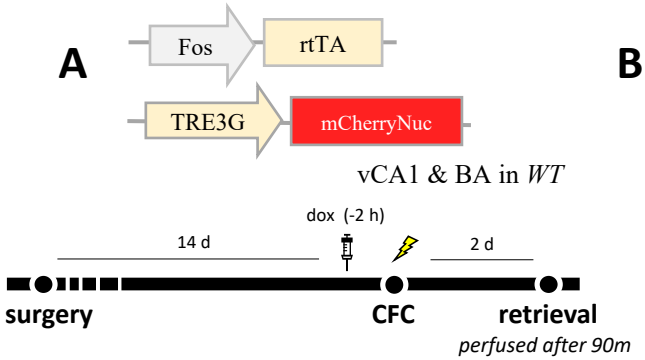
A
Fos
rtTA
TRE3G
mCherryNuc
vCA1 & BA in *WT*
dox (-2 h)
14 d
2 d
surgery
CFC
retrieval
perfused after 90m

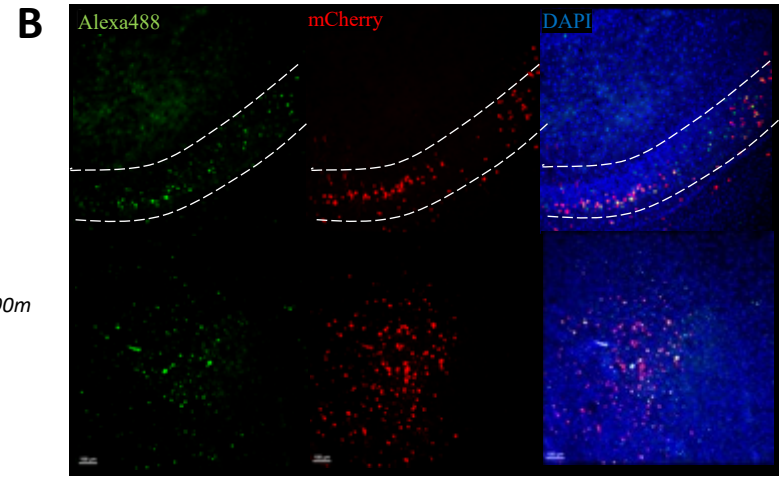
B
Alexa488
mCherry
DAPI

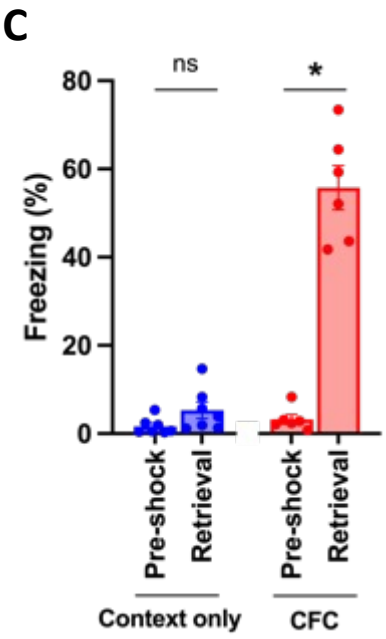
C
ns
*
Freezing (%)
80
60
40
20
0
Pre-shock
Retrieval
Pre-shock
Retrieval
Context only
CFC

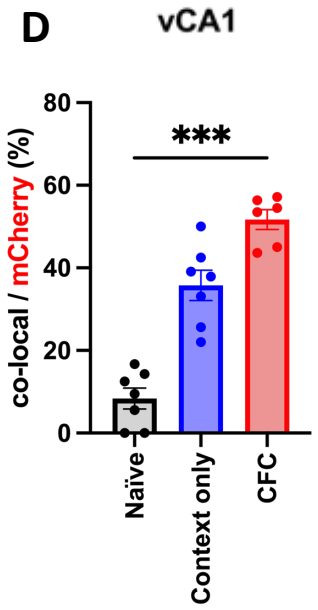
D
vCA1
***
co-local / mCherry (%)
80
60
40
20
0
Naïve
Context only
CFC

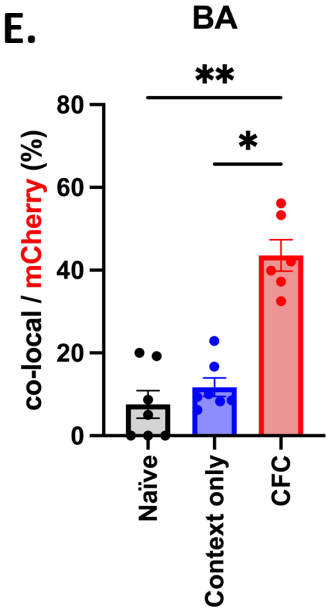
E.
BA
**
*
co-local / mCherry (%)
80
60
40
20
0
Naïve
Context only
CFC

Fig. S2

Fig S2. Engram reactivation of the vCA1 and BA during contextual fear conditioning.

(A) AAV1/2 containing Fos-rtTA/ TRE-mCherryNuc was injected into the vCA1 and BA of wild type mice.

(B) Representative image of the vCA1 (top) and BA (bottom). Neurons activated during the CFC were labelled in mCherry (middle) while neurons activated during memory retrieval were labelled in Alexa488 (left)

(C) Freezing level comparing between to pre-shock session and memory retrieval session. Context only group, N = 7; CFC group, N = 6. Wilcoxon test. *P = 0.0312. Data are presented as mean ± SEM.

(D-E) Reactivation ratio of engram cells in the vCA1 (**D**) and BA (**E**) in three groups: naïve, context only, and CFC. Naïve group, N = 7; context only group, N = 7; CFC group, N = 6. Wilcoxon test. ***P = 0.0002; **P = 0.0016; *P = 0.0256. Data are presented as mean ± SEM.

Fig. S3

A

	Pre-region	Post-region
	non engram	non engram
	engram	non engram
	non engram	engram
	engram	engram

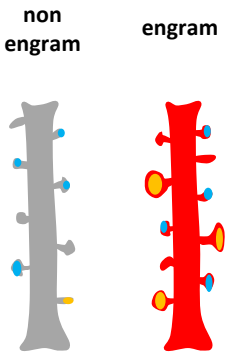

B

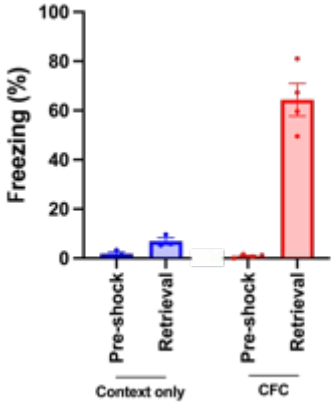

C

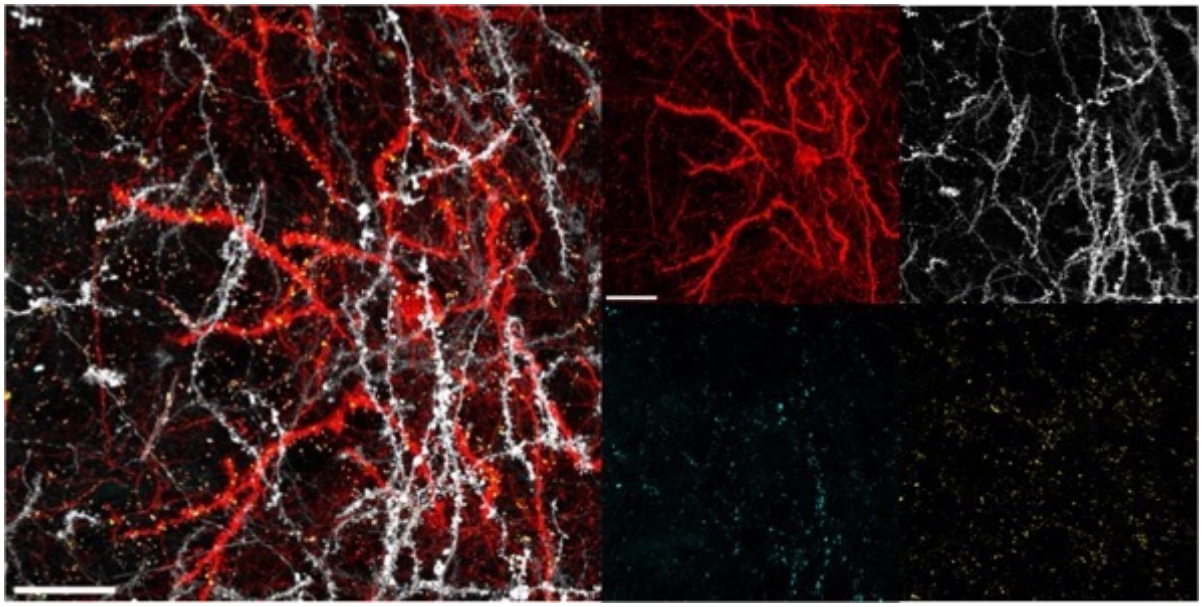

D

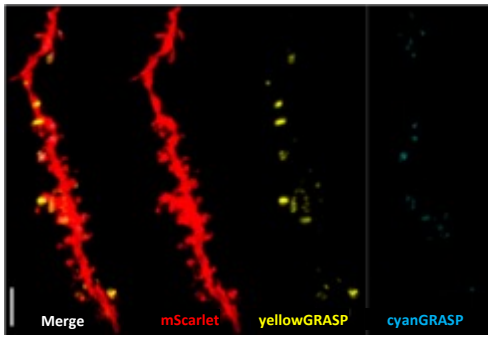

E

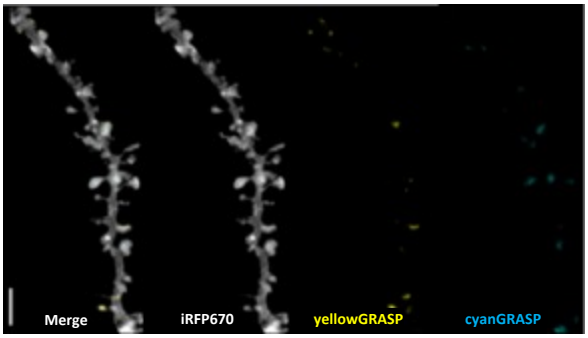

F

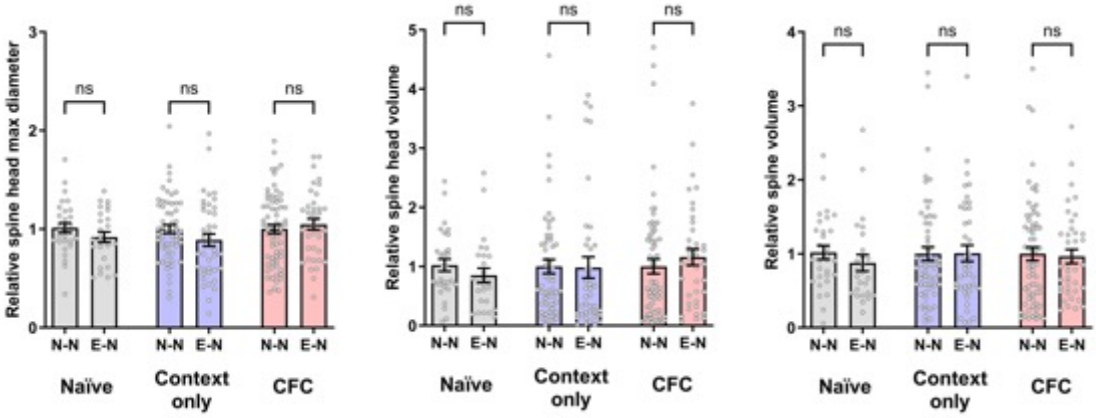

Fig S3.The overall synaptic connectivity from the vCA1 to the BA was not altered following the formation of memory.

(A) Categorisation of the four synaptic populations, represented by distinct colours.

(B) Freezing level during memory recall session for each group. Context only group, N = 3; CFC group, N = 4. Data are presented as mean ± SEM.

(C) Illustrative images depicting both engram (E) and nonengram (N) dendrites featuring GRASP signals in the BA. Scale bar : 30 μm

(D-E) Representative image of non-activated (D) and activated (E) GRASP signals displayed by each channel. Scale bar : 5 μm

(F) Normalised spine head diameters, spine head volume and spine volume of dendrites from BA non engram cells. Sizes of the spines with yellow puncta were normalised to those of the spines with cyan-only puncta of the same dendrite. Each data point represents a spine. Naïve group N-N, n = 30; E-N, n = 26; Context only group N-N, n = 57; E-N, n = 41; CFC group N-N, n = 66; E-N, n = 39. Two-way ANOVA followed by Tukey's multiple comparison test. Data are represented as mean ± SEM

Fig. S4

A

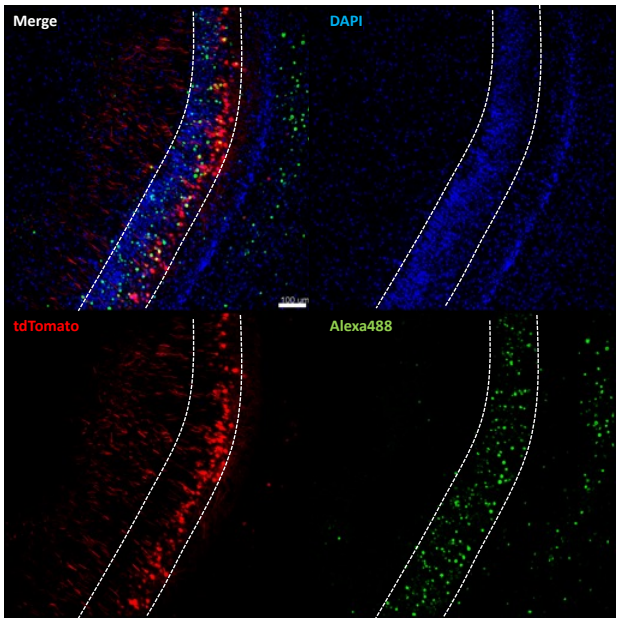

B

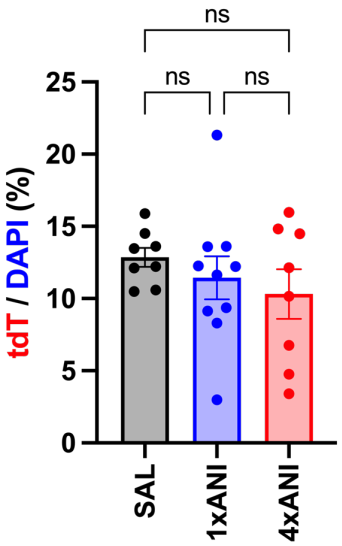

C

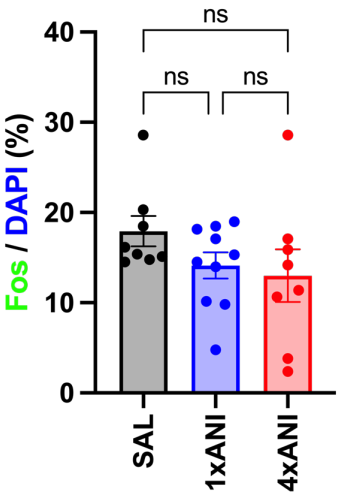

D

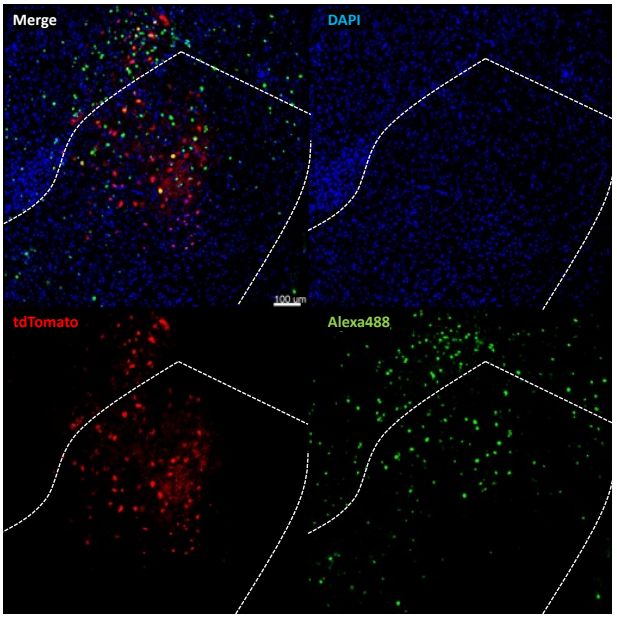

E

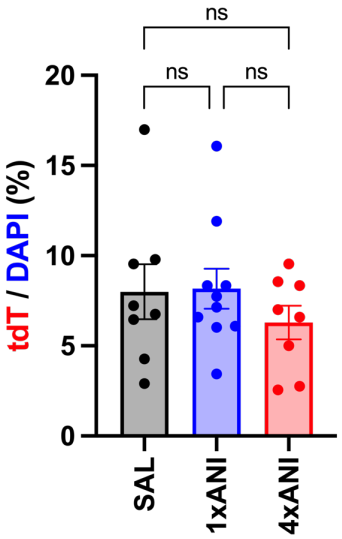

F

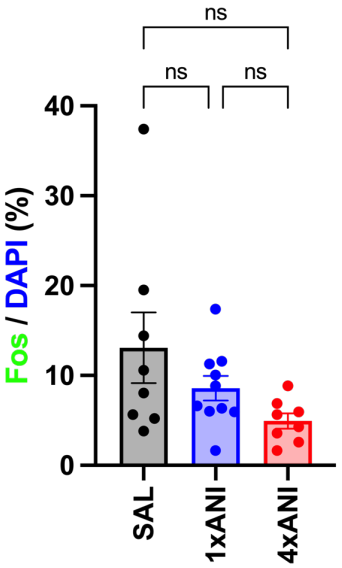

Fig S4. Engram labelling with PSI injections in Arc-TRAP mice.

(A) Representative images of activated neurones during the fear conditioning (tdTomato^{+}) in the vCA1 recall and neurones active during memory recall using cFos IHC (Alexa488). DAPI was stained to label the nuclei.

(B-C) cFos IHC result for the vCA1.

(D) Representative images of activated neurones during the fear conditioning (tdTomato^{+}) in the BA recall and neurones active during memory recall using cFos IHC (Alexa488). DAPI was stained to label the nuclei.

(D-E) cFos IHC result for the BA.

Fig. S5

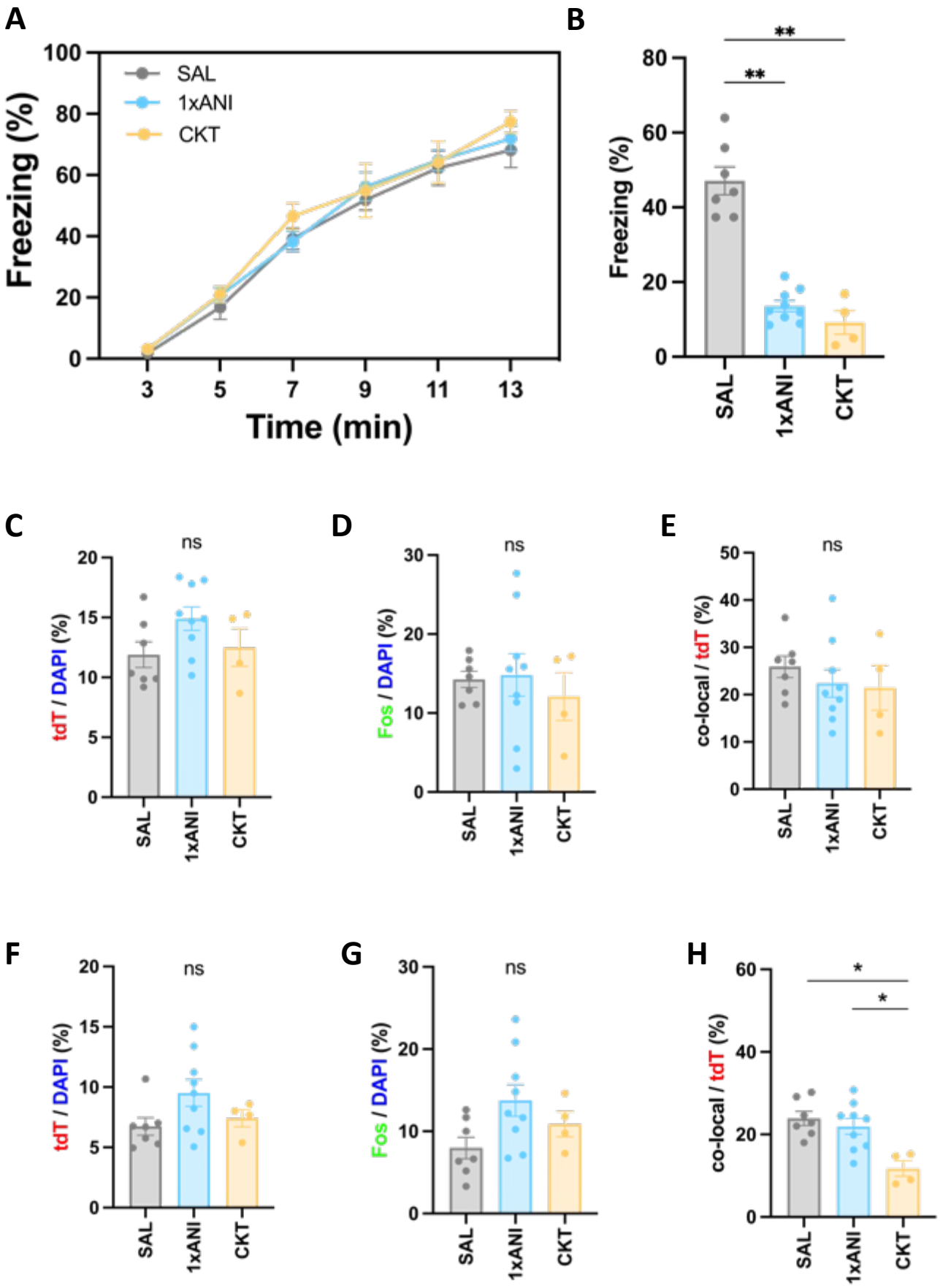
A
Freezing (%)
SAL
1xANI
CKT
Time (min)
B
Freezing (%)
**
**
SAL
1xANI
CKT
C
tdT / DAPI (%)
ns
D
Fos / DAPI (%)
ns
E
co-local / tdT (%)
ns
F
tdT / DAPI (%)
ns
G
Fos / DAPI (%)
ns
H
co-local / tdT (%)
*
*

Figure S5. Anisomycin combined with cycloheximide induced stronger retrograde amnesia.

(A) Acquisition plot for SAL, 1xANI, and CKT group during CFC. SAL group, N = 7; 1xANI group, N = 9; CKT group, N = 4. Data are presented as mean ± SEM.

(B) Freezing level during memory recall. Kruskal-Wallis test followed by Dunn's multiple comparison test. SAL vs. 1xANI, **P = 0.0067; SAL vs. CKT, **P = 0.0036. Data are presented as mean ± SEM.

(C-E) Immunohistochemistry data of vCA1. Kruskal-Wallis test followed by Dunn's multiple comparison test. Data are presented as mean ± SEM.

(F-H) Immunohistochemistry data of BA. Kruskal-Wallis test followed by Dunn's multiple comparison test. SAL vs. CKT, *P = 0.0148; 1xANI vs. CKT, *P = 0.0483. Data are presented as mean ± SEM.

Fig. S6

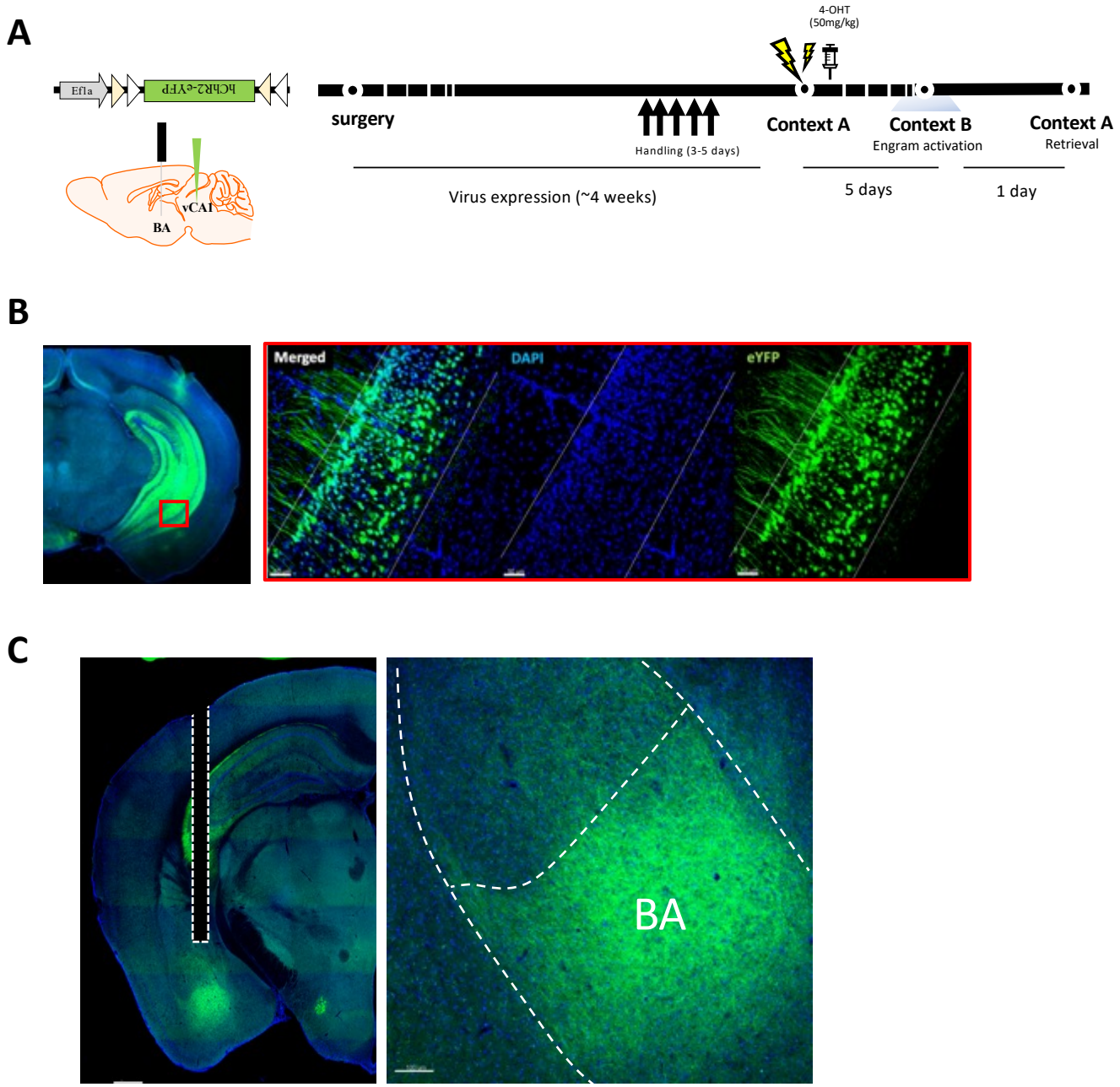

Fig S6. Representative images of virus expression for optogenetic behaviours. (**A**) Behavioural scheme (**B**) activated vCA1 neurones (**C**) vCA1 axonal projections to the BA expressed in ChR2-eYFP.

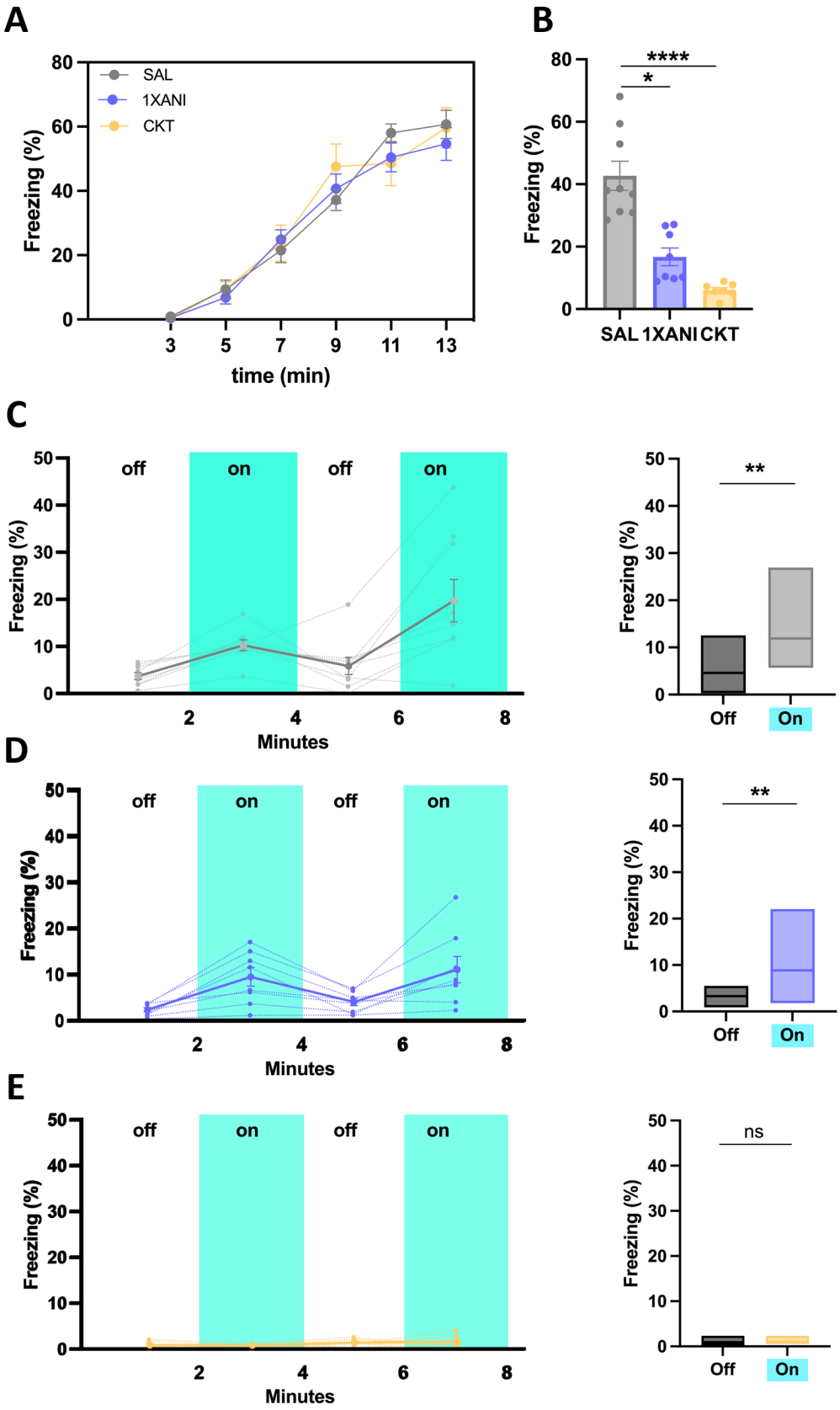
A
SAL
1XANI
CKT
Freezing (%)
time (min)
B
****
*
Freezing (%)
SAL
1XANI
CKT
C
off
on
off
on
Freezing (%)
Minutes
**
Off
On
D
off
on
off
on
Freezing (%)
Minutes
**
Off
On
E
off
on
off
on
Freezing (%)
Minutes
ns
Off
On

Fig S7. Memory cannot be artificially recalled when protein synthesis was blocked using combination of PSIs during memory acquisition.

(A) Freezing level during memory acquisition. Data are presented as mean ± SEM.

(B) Freezing level during contextual fear memory retrieval. SAL group, N = 9; 1xANI group, N = 8; CKT group, N = 7. Kruskal-Wallis test followed by Dunn's multiple comparison test. *P = 0.0380; ****P < 0.0003. Data are presented as mean ± SEM.

(C-E) Optogenetic activation of vCA1 engram axon terminals in BA of mice treated with different combination of PSI during memory acquisition. Mice expressing ChR2 in vCA1 engram cells show greater freezing during light-on epochs in saline-treated group (C) or by a single treatment of anisomycin (D) while absence of freezing behaviour was shown in mice treated with cocktail of PSI (E). Wilcoxon test. SAL group, **P = 0.0039; 1xANI group, **P = 0.0078. Data are presented as mean ± SEM (left) or median (right).

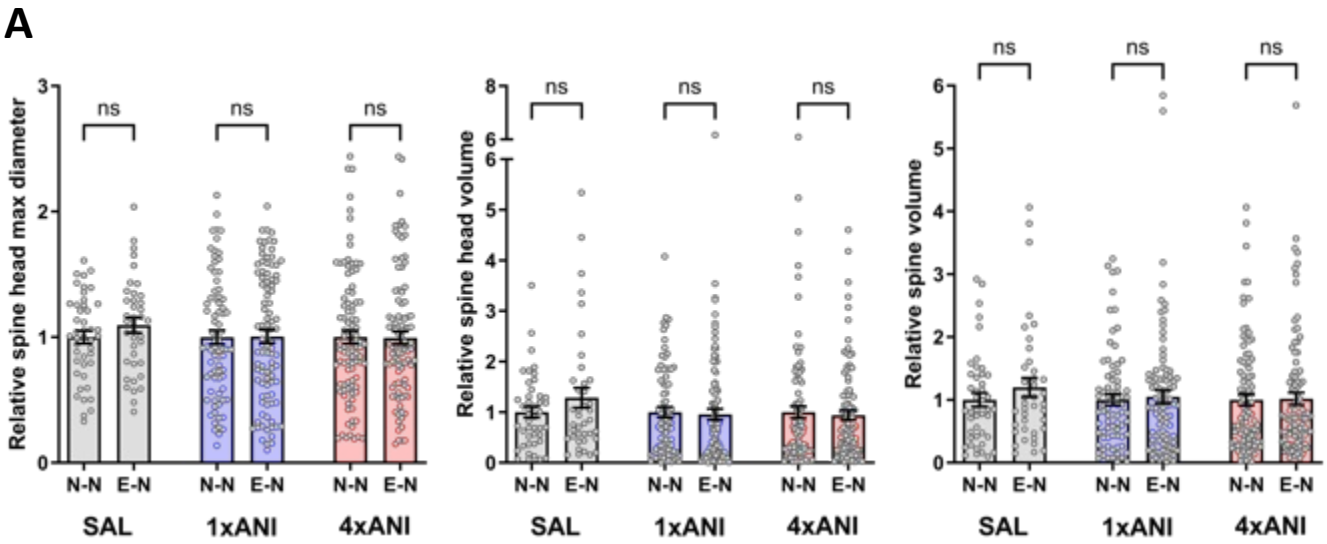

Fig S8. Normalised nonengram morphology after anisomycin treatment.

(A) Normalised spine head diameter, spine head volume and spine volume of dendrites from BA nonengram cells. SAL group N-N, $n = 44$; E-N, $n = 39$; 1xANI group N-N, $n = 77$; E-N, $n = 94$; 4xANI group N-N, $n = 96$; E-N, $n = 98$. Two-way ANOVA followed by Tukey's multiple comparison test. Data are presented as mean ± SEM.